

Investigation of Dust Ion Acoustic Shock and Solitary Waves in a Viscous Dusty Plasma

J. Goswami and S. S. Kausik*

Centre of Plasma Physics, Institute for Plasma Research,
Nazirakhat, Sonapur-782402, Kamrup (M), Assam, India.

*Corresponding author(s). E-mail(s): kausikss@rediffmail.com;

Abstract

A viscous dusty plasma containing Kappa- $(\kappa-)$ distributed electrons, positive warm viscous ions and constant negatively charged dust grains with viscosity have been considered to study the modes of dust-ion-acoustic waves (DIAWs) theoretically and numerically. The derivations and basic features of shock and solitary waves with different plasma parameters like Mach number, finite temperature coefficient, unperturbed dust streaming velocity, kinematic viscosity of dust etc. of this DIAWs mode have been performed. Considering the dynamical equation from Korteweg–de Vries(KdV) equation, a phase portrait has been drawn and the position of saddle point or col. and center have also been discussed. This type of dusty plasma can be found in celestial bodies. The results of this research work can be applied to study the properties of DIAWs in various astrophysical situation where κ -distributive electrons are present and careful modification of the same model can help us to understand the nature of the DIAWs of laboratory plasma as well.

Keywords: Reductive Perturbation Technique (RPT), KdV-Burgers Equation, Shock Waves, Solitary Waves, Phase Plane Analysis

1 Introduction

In the past few years, dusty plasmas or complex plasmas have become a topic of great research interest around the globe. It is a kind of plasma where nanometer or micrometer-sized particles are suspended. In most of the cases, these nanometer or micrometer sized particles known as dust are negatively charged

but there are various circumstances where they may be positively charged. The charge of dust particles varied in its size, greater the size of the dust particles larger its charge will be. Coupling via electrostatic force or any other forces like collision or viscous may happen and this coupling can change from weakly coupled to crystallising structures in the presence of these dust particles. The dependence of coupling parameter with the structural parameter has been discussed in detail by Dragan and Kutarov [1]. As we consider the density of dust particles is low, the viscosity is also very low, and no collision is being considered, so the effect of coupling is not taken into account in this present model like many other profound scientists did for dust ion acoustics waves (DIAWs) [2, 3]. Dusty plasma can be found in the celestial objects like comets, zodiacal dust cloud, interstellar, circumstellar clouds etc [4]. Not only astrophysical bodies but there are many examples of laboratory dusty plasma as well [4].

Depending on the motion of the species, dusty plasma can produce various waves, such as dust-acoustic waves (DAWs) [5], dust ion acoustic waves (DIAWs) [6]. We are going to consider dust ion acoustic waves (DIAWs) as the motion of both ions and dust species and also the distribution of electrons are taken into account. Some authors have mentioned the dust ion-acoustic waves term only by considering the motion of ions [7–14].

Furthermore, the ion-acoustic (IA) [15], electron acoustic (EA) [16] and electron-static (ES) [17] modes can also be present in a dusty plasma environment.

Also, shock waves in plasma have been found to have a greater interest in recent years. Various researchers have found many interesting results in the formation of shock waves in IA, EA, ES cases, and Laser Plasma Interactions (LPI) too [18]. Both theoretical and experimental study of shock waves has been found in recent years [19–22]. In the case of the production of shock waves in dusty plasma, there exists a good number of theoretical and experimental works [22–25]. Shock waves can be produced in plasma if there is a dissipative force present in the plasma. Two very important dissipative forces arise in the plasma due to collision and viscosity. These two forces cause the damping of plasma because of which shock waves have been formed.

In low density astrophysical plasma domain, there is deviation of the velocity distribution function (VDF) of particle from the Maxwellian distribution due to less number of binary collision among charges. Lorentzian velocity distribution function describes such superthermal particle distribution. Kappa distribution is one of these kinds of superthermal distribution where the particles have high-energy tails. This distribution can be given as [26, 27]-

$$f_{\kappa}^j(v) = \frac{n_{j0}\Gamma(\kappa+1)}{(\pi\kappa\theta^2)^{3/2}\Gamma(\kappa-\frac{1}{2})} \left[1 + \frac{v^2}{\kappa\theta^2}\right]^{-(\kappa+1)}.$$

Here, n_{j0} is the unperturbed particle density and $\theta^2 = \frac{(\kappa - \frac{3}{2})}{\kappa} \frac{2k_B T_j}{m_j}$. The effect of κ -distributive electrons have been shown by various researchers [28–30]. In the present paper, we have considered collisionless space plasma, and that is why we have taken kappa-distributed electrons. This type of distribution is frequently presented in collisionless space plasma [31].

At the time of the formation of the model of this present work, we have kept mainly two types of space plasma in our minds.

(a) Dusty plasma in an interstellar molecular cloud, a dense plasma, can consist of an H⁺ ion. In these types of dusty plasma, the normalized charge density of the dust grains is one ($q=1$). [32, 33].

and

(b) Dusty plasma is produced by the reaction of pickup H^+ ions and ambient plasma (i.e., solar wind) [34–36].

When physical parameters are varied there is a qualitative change in the behaviour of the system, these changes will be found in the Bifurcation analysis. Dynamical behaviours of nonlinear DIAWs in a magnetized dusty plasma has been reported by Samanta *et al.* [37].

In this work, the motion of ion and dust grains have been considered to construct this model and in both the cases kinematic viscosity is present. Also a finite temperature correction for the ions has also been taken in this model. As the time scale of the electrons is very much less than the other two species so we have taken a distribution for the electrons which is the kappa distribution. The work is performed in the weak non-linearity region and that is why we have used reductive perturbation technique (RPT). The momentum in the system are majorly supplied by the dust grains as it has heavier mass than ions and on the other hand the force in the system is majorly supplied by the ions. So keeping these things in mind we have derived the KdV-Burger and KdV equations for the system and most importantly discussed about the weak and strong shock in a DIAWs mode for the first time.

This paper is organised in the following way- in section 2 we have formulated the problem for the dusty plasma with the detailed discussion on kinematic viscosity and finite temperature correction in the ion in the following two subsections 2.1 and 2.2. In 3 we have linearized the dynamic equations given in 2 and achieved the linear dispersion relation for real and imaginary cases, as two dispersion relation arise here have the same form that is why we have discussed a general solution for both the equations in the subsection 3.1. In the next section 4 we have derived the KdV-Burger(KdVB) equation and in the subsection 4.1 we have solved the same. Afterward, under subsection 4.2, without considering the viscosity of both the species (dust grains and the ions), we have derived the KdV equation. The analytical and the numerical solution of the KdV equation have been achieved in subsections 4.2 and 4.3. Next, we have discussed the dynamic character and the stability of the KdVB equation in the section 5. Then we have discussed the results and discussion of the solution of KdVB and KdV equation which eventually giving us the shock

fronts and solitary structures in this section 6. Finally, in section 7 we give a brief summary of this paper.

2 Basic Formulations:

We have considered a unmagnetized dusty plasma in astrophysical space and investigated the dust-ion acoustic modes in such a plasma. As we have investigated the DIA mode, the dynamical equations for both ion and negative dust have been taken into account. The continuity equations for both the species is given by:

$$\frac{\partial n_j}{\partial t} + \frac{\partial (n_j u_j)}{\partial x} = 0, \quad (1)$$

here $j = d, i$. Now, the normalized momentum equation for the negative dust species in presence of the viscosity is given by

$$\frac{\partial u_d}{\partial t} + u_d \frac{\partial u_d}{\partial x} = q \frac{\partial \phi}{\partial x} + \eta_d \frac{\partial^2 u_d}{\partial x^2}. \quad (2)$$

The momentum equations for the ions is given by

$$\frac{\partial u_i}{\partial t} + u_i \frac{\partial u_i}{\partial x} = -\frac{\partial \phi}{\partial x} - 3\sigma n_i \frac{\partial n_i}{\partial x} - \eta_i \frac{\partial^2 u_i}{\partial x^2} \quad (3)$$

These continuity and momentum equations are bounded by the Poisson's equation which is given by,

$$\frac{\partial^2 \phi}{\partial x^2} = n_e - \delta n_i + q n_d \quad (4)$$

The electron has a super thermal distribution here in equation 4 and the electron density can be obtained after normalising and integrating the distribution over velocity space as,

$$n_e = n_{e0} \left\{ 1 - \frac{\phi}{(\kappa - \frac{3}{2})} \right\}^{-\kappa + \frac{1}{2}}. \quad (5)$$

All the other quantities have been discussed in the next three subsections 2.1-2.3.

2.1 The kinematic viscosity:

In the momentum equations for the negative dust and positive ion, we have considered that an effect of kinematic viscosity is present. It is a very special kind of viscosity depending predominately on the velocity of that species. Coefficient of absolute viscosity (μ) is basically the measurement of internal resistance. A force is generated due to this internal resistance and is given by $F = \mu A \times S$, where A surface area of the plasma and S is shear rate in the

plasma. This law of the force is known as “Newton’s law of viscosity”. In the equations 2 and 3, the viscosity we use is the kinematic viscosity as we mention earlier and this is basically the ratio between absolute viscosity (μ) and fluid mass density (n), this is previously discussed by Goswami and Sarkar [38].

2.2 The finite temperature correction in the ion:

The second term in the right hand side of the momentum equation of ion (equation 3) arises due to the finite temperature correction [39, 40]. This finite temperature correction in the system only arises when the ions are going to follow the Fermi-Dirac (FD) statics. As ions are very much lighter than the dust particle then the quantum mechanical tunneling effect comes into act and we have to consider that the chemical potential (μ_c) remains constant due to non-equilibrium dynamics. Considering all these, the non-equilibrium particle density is given by the following equation:

$$n_0 = \frac{1}{2\pi^2} \left(\frac{2m}{\hbar} \right)^2 \int_0^\infty \frac{E^{1/2} dE}{e^{\beta(E-\mu_c)} + 1}$$

where m is the mass of the ion, \hbar is the reduced Planck constant, n_0 is the equilibrium number density, $\beta = \frac{1}{k_B T_{i0}}$, T_{i0} is the back-ground temperature of ion and μ_c is the chemical potential. Applying this pressure term without considering the Bohm diffraction term we get the equation 3. Following the same procedure as used by Akbari-Moghanjoughi and Eliasson [41] and Goswami *et al.* [17] we get the σ as

$$\sigma = \frac{L_{5/2}(-e^{\beta\mu_c})}{L_{3/2}(-e^{\beta\mu_c})} \left(\frac{V_{Ti}}{V_{Fi}} \right)^2.$$

Here $Li_\nu(x)$ is the polylogarithmic function in x of the order ν .

Some of the authors [42, 43] consider the plasma as a Fermi gas so the pressure is:

$$p_i = \frac{1}{3} \frac{mv_{Fi}^2}{n_{i0}^2} n_i^3$$

And in this model if we consider this pressure then it will only be present in case of the ion as it is lighter than the dust species. Considering this pressure, our momentum equation 3 would look like,

$$\frac{\partial u_i}{\partial t} + u_i \frac{\partial u_i}{\partial x} = -\frac{\partial \phi}{\partial x} - \sigma_i n_i \frac{\partial n_i}{\partial x} - \eta_i \frac{\partial^2 u_i}{\partial x^2}$$

where σ_i is the ratio between ion to electron Fermi temperature.

2.3 Normalization Schemes and Charge Neutrality

From equations 1-4, all the equations are normalized and the standard normalization schemes are given by: $\hat{x} \rightarrow \frac{x}{\lambda_D}$, $\hat{t} \rightarrow \omega_p t$, $\hat{\phi} \rightarrow \frac{e\phi}{T_i}$, $\hat{u}_j \rightarrow \frac{u_j}{v_{Te}}$,

and $\hat{\eta}_j \rightarrow \frac{\eta_j}{\lambda_D v_{Te}}$. Also, at the equilibrium the charge neutrality condition is $n_{e0} + qn_{d0} = \delta n_{i0}$. Generally, plasma parameters have effects on the function of dust charge. But dust-ion acoustic (DIA) time scale is much shorter than the dust charging time scale. Thus, we can clearly assumed that in DIA mode there is no significant effect of dust charge fluctuation. Therefore, the dust charge can be assumed to be constant [44, 45]. In this manuscript we have all along taken ' $q = 1$ '. The various values of this dust charges in different astrophysical plasmas have been discussed by EL-Labany *et al.* [32].

3 Linear Dispersion Relation:

In order to investigate the linear and nonlinear behavior of dust acoustic wave in this three-component electron-ion-dust plasma, we make the following perturbation expansion for the field quantities n_j , u_j and ϕ about their equilibrium values:

$$\begin{bmatrix} n_j \\ u_j \\ \phi \end{bmatrix} = \begin{bmatrix} 1 \\ u_{j0} \\ \phi_0 \end{bmatrix} + \varepsilon \begin{bmatrix} n_j^{(1)} \\ u_j^{(1)} \\ \phi^{(1)} \end{bmatrix} + \varepsilon^2 \begin{bmatrix} n_j^{(2)} \\ u_j^{(2)} \\ \phi^{(2)} \end{bmatrix} + \dots \quad (6)$$

We assumed that all field variables varying as $\exp[i(kx - \omega t)]$ and here ω is the normalized wave frequency and k is the wave number, which contains both real(k_r) and imaginary part(k_i). Here, the viscous term plays a very pivotal role. The dispersion equation has an exponentially decaying complex part in addition to the real dispersion relation. In this case if we substitute the wave number with a real plus imaginary parts(given by $k = k_r + ik_i$), we obtain the two dispersion relations as given below.

The real dispersion relation is given by,

$$P_1\omega'^4 + Q_1\omega'^3 + R_1\omega'^2 + S_1\omega' + T_1 = 0, \quad (7)$$

where,

$$\left. \begin{aligned} P_1 &= - \left[k_r^2 + \frac{1 - 2\kappa}{2\kappa - 3} \right] \\ Q_1 &= -2k_r P_1 (u_{i0} + u_{d0}) \\ R_1 &= P_1 [4k_r^2 u_{i0} u_{d0} + k_r^2 u_{d0}^2 + k_r^2 u_{i0}^2 + 3\sigma k_r^2] + 2k_r^2 (\delta + q^2) \\ S_1 &= -P (2k_r^3 u_{i0} u_{d0}^2 + 2k_r^3 u_{i0}^2 u_{d0} + 6k_r^3 \sigma u_{d0}) + 2k_r^3 (\delta + q^2) (u_{d0} + u_{i0}) \\ T_1 &= P_1 (k_r^4 u_{i0}^2 u_{d0}^2 + 3\sigma k_r^4 u_{d0}^2) - k_r^4 (\delta + q^2) (u_{i0}^2 u_{d0}^2 + 3\sigma) \end{aligned} \right\} \quad (8)$$

The imaginary dispersion relation is given by,

$$P_2\omega''^4 + Q_2\omega''^3 + R_2\omega''^2 + S_2\omega'' + T_2 = 0, \quad (9)$$

where,

$$\left. \begin{aligned} P_2 &= - \left[k_i^2 + \frac{1 - 2\kappa}{2\kappa - 3} \right] \\ Q_2 &= P_2 k_i^2 \\ R_2 &= -P_2 (3\sigma k_i^2 - \eta_{ii} \eta_{di} k_i^4) - 2k_i^2 (\delta + q^2) \\ S_2 &= -3P_2 \sigma \eta_{di} k_i^4 + k_i^4 (\delta + q^2) (\eta_{di} - \eta_{ii}) \\ T_2 &= -3\sigma k_i^4 (\delta + q^2) \end{aligned} \right\} \quad (10)$$

3.1 General Solution:

These two equation (7) and (9) have the same form the solution of these kind of equation is given below; The dispersion relations have the form

$$P\omega^4 + Q\omega^3 + R\omega^2 + S\omega + T = 0, \quad (11)$$

or,

$$\omega^4 + \frac{Q}{P}\omega^3 + \frac{R}{P}\omega^2 + \frac{S}{P}\omega + \frac{T}{P} = 0, \quad (12)$$

or,

$$\omega^4 + Q_3\omega^3 + R_3\omega^2 + S_3\omega + T_3 = 0, \quad (13)$$

Let, $\omega = x - \frac{Q_3}{4}$ then the above equation becomes,

$$x^4 + px^2 + qx + r = 0, \quad (14)$$

where,

$$\left. \begin{aligned} p &= -\frac{6Q_3^2}{16} - \frac{3Q_3}{4} + R_3 \\ q &= \frac{Q_3^3}{8} - \frac{2Q_3R_3}{4} + S_3 \\ r &= -\frac{3Q_3^4}{256} + \frac{Q_3^2R_3}{16} - \frac{Q_3}{4} + T_3 \end{aligned} \right\} \quad (15)$$

From equation (14)

$$\left(x^2 + \frac{p}{2}\right)^2 = -qx - r + \left(\frac{p}{2}\right)^2 \quad (16)$$

or,

$$\left(x^2 + \frac{p}{2} + u\right)^2 = -qx - r + \left(\frac{p}{2}\right)^2 + 2ux^2 + pu + u^2 \quad (17)$$

In order to have perfect square, we have,

$$8u^3 + 8pu^2 + (2p^2 - 8r)u - q^2 = 0 \quad (18)$$

or,

$$u^3 + pu^2 + \left(\frac{2p^2 - 8r}{8}\right)u - \frac{q^2}{8} = 0 \quad (19)$$

or,

$$u^3 + pu^2 + lu + g = 0, \quad (20)$$

where, $l = \left(\frac{2p^2 - 8r}{8}\right)$ and $g = -\frac{q^2}{8}$.

Again, let $u = t - \frac{p}{3}$ equation yields

$$t^3 + jt + l = 0, \quad (21)$$

where, $j = \frac{3l - p^2}{3}$ and $l = \frac{2p^3 - 9pl + 27g}{27}$. Solution of this equation is,

$$t = \left(-\frac{l}{2} + \sqrt{\frac{l^2}{4} + \frac{j^3}{27}}\right)^{1/3} + \left(-\frac{l}{2} - \sqrt{\frac{l^2}{4} + \frac{j^3}{27}}\right)^{1/3} \quad (22)$$

Now, we know $u = t - \frac{p}{3}$ the equation transforms into

$$x^2 + \frac{p}{2} + u = \pm \left[\sqrt{2u} - \frac{2}{2\sqrt{2u}} \right] \quad (23)$$

Solving this equation we get,

$$x = \pm \sqrt{-\frac{p}{2} - u \pm \left[\sqrt{2u} - \frac{2}{2\sqrt{2u}} \right]} \quad (24)$$

Therefore we get,

$$\omega = -\frac{Q_3}{4} + x \quad (25)$$

This equation (25) is the general solution for the equations (7) and (9). Clearly this general solution has four roots that means the real dispersion relation (equation 7) and the imaginary dispersion relation (equation 9) individually have four roots. Under these four roots in each cases two roots are physically admissible [46]. Again in these two roots for each of the cases we can categorize them as ‘fast’ and ‘slow’ mode.

4 Derivation of KdV-Burgers Equation:

In order to derive the equation of motion for the nonlinear dust ion acoustic wave, we employ the reductive perturbation technique and define the following stretched variables,

$$\left. \begin{aligned} \xi &= \varepsilon^{1/2} (x - Mt) \\ \tau &= \varepsilon^{3/2} t \\ \eta &= \varepsilon^{1/2} \eta_0 \end{aligned} \right\} \quad (26)$$

where ε is a small parameter which characterizes the strength of nonlinearity, and M is the Mach number i.e. the phase velocity of the wave. The stretching in η is due to the small variations in perpendicular directions.

Now, Eqs (1-4) are written in terms of the stretched coordinates ξ , τ , and η and substituting the perturbation expansion given in Eq. (26). From these equations equating the lowest orders in ε (i.e., $\varepsilon^{3/2}$) with the boundary conditions that all variables, that is, $n_i^{(1)}$, $u_i^{(1)}$, $n_d^{(1)}$, $u_d^{(1)}$ and $\phi^{(1)}$ tend to zero as $\xi \rightarrow \pm\infty$, we get,

$$\left. \begin{aligned} u_d^{(1)} &= -\frac{q}{(M - u_{d0})} \phi^{(1)} \\ n_d^{(1)} &= -\frac{q}{(M - u_{d0})^2} \phi^{(1)} \\ u_i^{(1)} &= \frac{\phi^{(1)} (M - u_{di})}{(M - u_{di})^2 - 3\sigma} \\ n_d^{(1)} &= \frac{\phi^{(1)}}{(M - u_{di})^2 - 3\sigma} \end{aligned} \right\} \quad (27)$$

Going to next higher order terms in ε , that is, $\varepsilon^{5/2}$ -th term, we get,

$$(M - u_{d0}) \frac{\partial n_d^{(2)}}{\partial \xi} = \frac{\partial u_d^{(2)}}{\partial \xi} - \frac{q}{(M - u_{d0})^2} \frac{\partial \phi^{(1)}}{\partial \tau} + \frac{q^2}{(M - u_{d0})^3} \frac{\partial \phi^{(1)^2}}{\partial \xi} \quad (28)$$

$$\begin{aligned} (M - u_{i0}) \frac{\partial n_i^{(2)}}{\partial \xi} &= \frac{\partial u_i^{(2)}}{\partial \xi} - \frac{1}{[(M - u_{i0})^2 - 3\sigma]} \frac{\partial \phi^{(1)}}{\partial \tau} \\ &+ \frac{(M - u_{i0})}{[(M - u_{i0})^2 - 3\sigma]} \frac{\partial \phi^{(1)^2}}{\partial \xi} \end{aligned} \quad (29)$$

$$\begin{aligned} \frac{\partial u_d^{(2)}}{\partial \xi} &= -\frac{q}{(M - u_{d0})^2} \frac{\partial \phi^{(1)}}{\partial \tau} + \frac{q^2}{(M - u_{d0})^3} \frac{\partial \phi^{(1)}}{\partial \xi} \\ &- \frac{q}{(M - u_{d0})^2} \frac{\partial \phi^{(2)}}{\partial \xi} + \frac{q\eta_{d0}}{(M - u_{d0})^2} \frac{\partial^2 \phi^{(1)}}{\partial \xi^2} \end{aligned} \quad (30)$$

$$\begin{aligned}
\frac{\partial u_i^{(2)}}{\partial \xi} &= \frac{1}{M - u_{i0}} \frac{\partial \phi^{(2)}}{\partial \xi} + \frac{1}{\left[(M - u_{i0})^2 - 3\sigma\right]} \frac{\partial \phi^{(1)}}{\partial \tau} \\
&+ \frac{\left[3(M - u_{i0})^2 - 3\sigma\right]}{(M - u_{i0}) \left[(M - u_{i0})^2 - 3\sigma\right]^2} \phi^{(1)} \frac{\partial \phi^{(1)}}{\partial \xi} \\
&+ \frac{3\sigma}{(M - u_{i0})} \frac{\partial n_i^{(2)}}{\partial \xi} + \frac{\eta_{i0}}{\left[(M - u_{i0})^2 - 3\sigma\right]} \frac{\partial^2 \phi^{(1)}}{\partial \xi^2}
\end{aligned} \tag{31}$$

The second-order perturbation of the Poisson's equation can be equated as

$$\frac{\partial^2 \phi^{(1)}}{\partial \xi^2} = \left[\frac{1 - 2\kappa}{2\kappa - 3} + \frac{(4\kappa^2 - 1)}{(2\kappa - 3)^2} \right] \phi^{(2)} + \frac{(4\kappa^2 - 1)}{2(2\kappa - 3)^2} \phi^{(1)2} - \delta n_i^{(2)} + q n_d^{(2)} \tag{32}$$

Differentiating both sides of Eq. (32) by ξ and carrying out a detailed algebraic treatment with the Equations from (28) to (31), the nonlinear KdV–Burgers equation is given by the following equation

$$\frac{\partial \phi^{(1)}}{\partial \tau} + A \phi^{(1)} \frac{\partial \phi^{(1)}}{\partial \xi} + B \frac{\partial^3 \phi^{(1)}}{\partial \xi^3} + C \frac{\partial^2 \phi^{(1)}}{\partial \xi^2} = 0 \tag{33}$$

where, $A = \frac{\Gamma}{\Theta}$, $B = \frac{1}{\Theta}$ and $C = \frac{\Upsilon}{\Theta}$. The Γ , Θ and Υ are given below.

$$\left. \begin{aligned}
\Gamma &= \frac{3\delta \left[(M - u_{i0}) + \sigma\right]}{\left[(M - u_{i0})^2 - 3\sigma\right]^3} - \frac{3q^3}{(M - u_{d0})^4} - \frac{4\kappa^2 - 1}{(2\kappa - 3)^2} \\
\Theta &= \frac{2(M - u_{i0})\delta}{\left[(M - u_{i0})^2 - 3\sigma\right]^2} + \frac{2q^2}{(M - u_{d0})^2} \\
\Upsilon &= \frac{\eta_{i0}(M - u_{i0})\delta}{\left[(M - u_{i0})^2 - 3\sigma\right]^2} - \frac{\eta_{d0}q^2}{(M - u_{d0})^3}
\end{aligned} \right\} \tag{34}$$

The nonlinear equation (33) is the well known KdV–Burgers(KDVB) equation and the coefficients A , B and C are the nonlinear, dispersive and dissipative coefficients, respectively.

4.1 Solution of KdVBurgers Equation:

The equation (33) is nonlinear equation in both the variables ξ a space like variable and τ a time like variable. To solve this equation we have to first join these variables into one wave variable $\psi = \xi - M\tau$ to transform the partial differential equation (PDE) of two variables ξ and τ into ordinary differential equation (ODE) of one variable ψ with the application of the boundary

conditions when $\psi \rightarrow 0$ then $\phi^{(1)} \rightarrow 0$ and $\frac{\partial \phi^{(1)}}{\partial \psi} \rightarrow 0$ as [17, 47, 48]

$$-M \frac{d\phi^{(1)}}{d\psi} + A\phi^{(1)} \frac{d\phi^{(1)}}{d\psi} + B \frac{d^2 \phi^{(1)}}{d\psi^2} + C \frac{d^3 \phi^{(1)}}{d\psi^3} \quad (35)$$

As we are trying to solve this equation with the help of tan-hyperbolic method so now we have to take $s = \tanh \psi$ and assuming a series solution predicted by Wazwaz [49] as $\phi^{(1)}(s) = \sum_{j=0}^n a_j s^j$ and we get the following solution,

$$\phi^{(1)} = \frac{12A}{B} [1 - \tanh^2(\psi)] - \frac{36C}{15A} \tanh(\psi) \quad (36)$$

This equation (36) is the solution of the KdVB equation (33).

4.2 The KdV equation and the solution:

It is very clear that if there is no viscous force considered for both the species, i.e. ion and dust then $\eta_{i0} = \eta_{d0} = 0$. So there will be no dissipation and $C = 0$. In this condition, the equation (33) is transformed into Korteweg de Vries (KdV) equation.

$$\frac{\partial \phi^{(1)}}{\partial \tau} + A\phi^{(1)} \frac{\partial \phi^{(1)}}{\partial \xi} + B \frac{\partial^3 \phi^{(1)}}{\partial \xi^3} \quad (37)$$

The coefficients A and B are already given. Using the same transformation $\psi = \xi - M\tau$ and the boundary condition we have the solution of the KdV equation,

$$\phi^{(1)} = \phi_0 \operatorname{sech}^2 \left(\frac{\psi}{\Delta} \right) \quad (38)$$

where, $\phi_0 = \frac{3M}{A}$ and $\Delta = 2\sqrt{\frac{M}{C}}$

4.3 Numerical solution of KdV:

Following the same procedure as Soliman, Ali and Raslan [50], we find out the numerical solution of the KdV equation. Taking $F = A \frac{\phi^{(1)2}}{2} + B \frac{\partial^2 \phi^{(1)}}{\partial \xi^2}$ the equation (37) transforms into the given form

$$\frac{\partial \phi^{(1)}}{\partial \tau} + \frac{\partial F}{\partial \xi} = 0 \quad (39)$$

Using the finite difference method the equation (39) becomes,

$$\frac{\phi_i^{(1)n+1} - \phi_i^{(1)n}}{\Delta \tau} + \frac{F_{i+\frac{1}{2}} - F_{i-\frac{1}{2}}}{\Delta \xi} = 0 \quad (40)$$

Using the similarity solution procedure we can have the solution of equation (37) as follows (representing the $\phi^{(1)}$ as ϕ here),

$$\begin{aligned} \phi_i^{n+1} = \phi_i^n - \frac{\Delta\tau}{\Delta\xi} \left[\frac{A}{4} \left\{ (\phi_{i+1} - (\Phi_x)_{i+1}H + (\Phi_{xx})_{i+1}M_1)^2 \right. \right. \\ \left. \left. + (\phi_i + (\Phi_x)_iH + (\Phi_{xx})_iM_1)^2 - (\phi_i - (\Phi_x)_iH + (\Phi_{xx})_iM_1)^2 \right. \right. \\ \left. \left. - (\phi_{i-1} - (\Phi_x)_{i-1}H + (\Phi_{xx})_{i-1}M_1)^2 \right\} \right. \\ \left. + \frac{B}{2} \left\{ b^2(\Phi_x)_{i+1}H + (\Phi_{xx})_{i+1}H + (\Phi_{xx})_{i+1}M_2 - b^2(U_x)_iH + (\Phi_{xx})_iM_2 \right. \right. \\ \left. \left. - b^2(\Phi_x)_iH - (\Phi_{xx})_{i+1}M_2 + b^2(\Phi_x)_{i-1}H - (\Phi_{xx})_{i-1}M_2 \right\} \right] \end{aligned} \quad (41)$$

Here,

$$\left. \begin{aligned} H &= \frac{1}{4\cos\alpha} \\ M_1 &= -\frac{\cos\alpha - 1}{4\sin\alpha} \\ M_2 &= \frac{b^2\cos\alpha}{4\sin^2\alpha} \end{aligned} \right\} \quad (42)$$

where,

$$\left. \begin{aligned} \alpha &= \frac{1}{2}b\Delta\xi \\ \beta &= bM\Delta\tau \end{aligned} \right\} \quad (43)$$

also

$$b = \sqrt{\frac{M + AD}{B}} \quad (44)$$

and also

$$\left. \begin{aligned} \Phi_{xx} &= \phi_{i+1}^n - 2\phi_i^n + \phi_{i-1}^n \\ \Phi_x &= \phi_{i+1}^n - \phi_{i-1}^n \end{aligned} \right\} \quad (45)$$

Here, D is the local similarity equation.

5 Phase Plane Analysis:

In this section, we transform the KdV equation (37) into a dynamical system with the help of $\chi = \xi - v\tau$ and $\phi^{(1)}(\xi, \tau) = \phi^{(1)}(\chi)$

$$\left. \begin{aligned} \frac{d\phi^{(1)}}{d\chi} &= z \\ \frac{dz}{d\chi} &= \frac{v}{B}\phi^{(1)} - \frac{A}{B}\phi^{(1)2} \end{aligned} \right\}. \quad (46)$$

To locate critical points by solving the equations $\dot{\phi} = \dot{z} = 0$, ‘ \cdot ’ sign represents $\frac{d}{d\chi}$.

Hence, $\dot{\phi} = 0$ if $z = 0$ and $\dot{z} = 0$ if $(\frac{v}{B}\phi - \frac{A}{B}\phi^2) = 0$.

If $z = 0$ then $\dot{z} = 0$ if $(\frac{v}{B}\phi - \frac{A}{B}\phi^2) = 0$ which has two solutions, $\phi = 0$ and $\phi = \frac{v}{A}$. Therefore, there are two critical points $(0, 0)$ and $(\frac{v}{A}, 0)$.

Linearize by finding the Jacobian matrix; hence,

$$J = \begin{pmatrix} 0 & 1 \\ \frac{v}{B} - \frac{2A}{B}\phi & -\frac{C}{B} \end{pmatrix} \quad (47)$$

Linearizing in first critical point that is $(0, 0)$ we get,

$$J_{(0,0)} = \begin{pmatrix} 0 & 1 \\ \frac{v}{B} & -\frac{C}{B} \end{pmatrix} \quad (48)$$

The Eigen values for this Jacobian are $\lambda = \frac{-\frac{C}{B} \pm \sqrt{\frac{C^2}{B^2} + \frac{4v}{B}}}{2}$. Again, linearizing in second critical point that is $(\frac{v}{A}, 0)$ we get,

$$J_{(\frac{v}{A}, 0)} = \begin{pmatrix} 0 & 1 \\ -\frac{v}{B} & -\frac{C}{B} \end{pmatrix} \quad (49)$$

And the eigenvalues for this Jacobian are $\lambda = \frac{-\frac{C}{B} \pm \sqrt{\frac{C^2}{B^2} - \frac{4v}{B}}}{2}$.

From the eigenvalues at the two critical points it is clear that for the critical point $(0, 0)$ the eigenvalues are always real as the dispersive coefficient B is always positive in this model but there is a possibility that the eigenvalues for the critical point $(\frac{v}{A}, 0)$ can be imaginary if $\frac{4v}{B} > \frac{C^2}{B^2}$.

The dynamical system [46](#) are Hamiltonian system are Hamiltonian system of the Hamiltonian function,

$$H(\phi, z) = \frac{z^2}{2} - \frac{v\phi^2}{2B} - \frac{A\phi^3}{3B} \quad (50)$$

This is obviously a two dimensional Hamiltonian function.

From the nature of the Jacobian and the eigenvalues, we categorize these critical points in two distinct category.

(i) At equilibrium point or critical point E_0

$$D = \det J_{(0,0)} = \begin{vmatrix} 0 & 1 \\ \frac{v}{B} & -\frac{C}{B} \end{vmatrix} = -\frac{v}{B} < 0 \quad (51)$$

which implies E_0 is a saddle point.

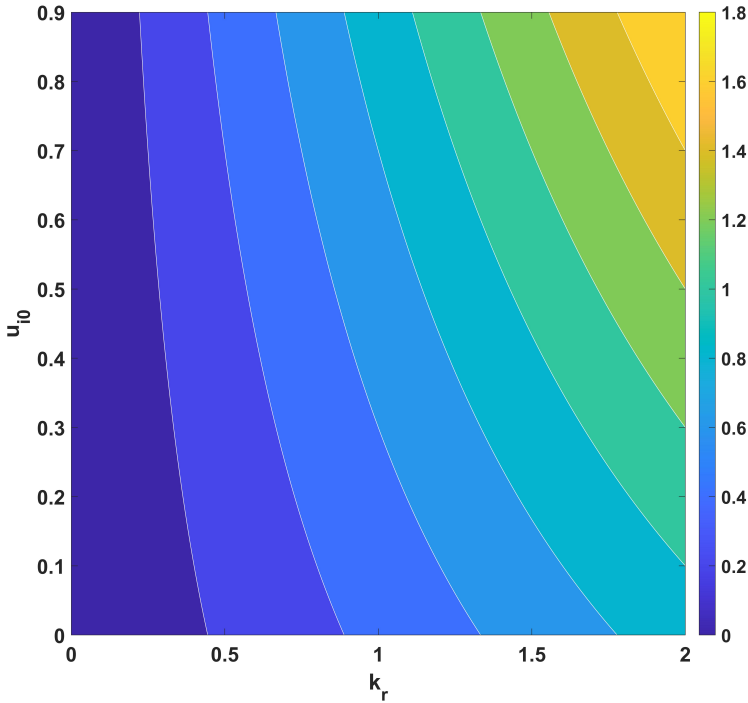


Fig. 1 Contour plot of one root of ω' , carrier wave number k_r and unperturbed ion streaming velocity u_{i0} with unperturbed dust streaming velocity (u_{d0}) = 0.07, finite temperature coefficient (σ) = 0.65, kappa index (κ) = 5 and dust charge (q) = 1

(ii) At equilibrium/ critical point E_1 i.e. $(\frac{v}{A}, 0)$

$$D = \det J_{(0,0)} = \begin{vmatrix} 0 & 1 \\ -\frac{v}{B} & -\frac{C}{B} \end{vmatrix} = \frac{v}{B} > 0 \quad (52)$$

which implies E_1 is a center.

The trace of both the determinate is same which is $-\frac{C}{B} > 0$, as C itself is a negative quantity.

6 Results:

In the section 4, we have derived and analyse various linear and nonlinear effect in this plasma model analytically and numerically. At first we will discuss about the variation of the one root of the real dispersion relation with various ion streaming velocity in the figure 1. In this contour plot we can see that the nonlinear damping rate increases as the unperturbed ion velocity (u_{i0}) increases. Next, in the figure 2 we have discussed the variation of one imaginary root of the imaginary dispersion relation expressed in the equation 9. This is also a contour plot but the nature of it is totally different from the previous one (figure 1). This change in nature have two possible reasons. Firstly, in the

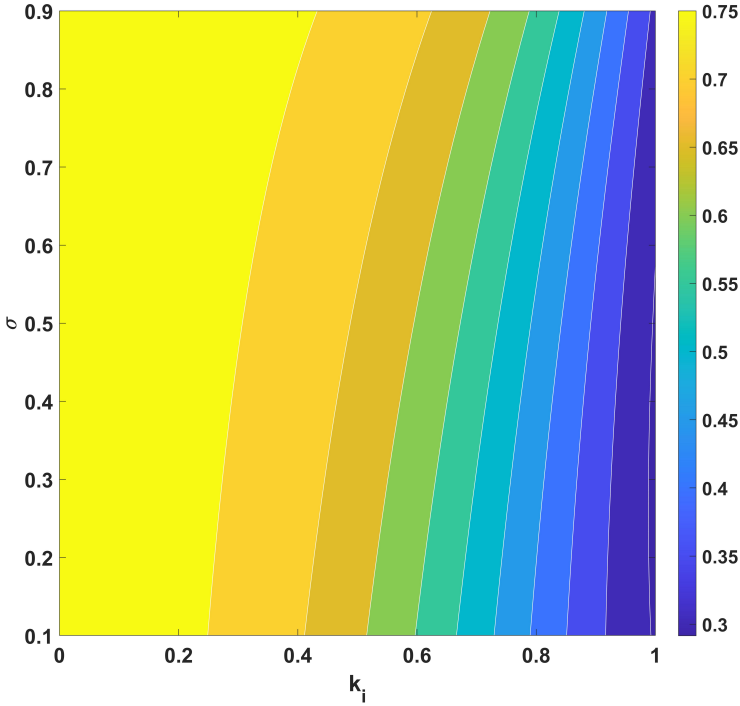


Fig. 2 Contour plot of one root of ω'' , carrier wave number k_i and finite temperature coefficient (σ) with kinematic viscosity of ion (η_{i0}) = 0.09, kinematic viscosity of dust (η_{d0}) = 0.07, finite temperature coefficient (σ) = 0.65, kappa index (κ) = 5 and dust charge (q) = 1

calculation of imaginary dispersion relation 9 we do not consider the streaming velocity of ions and the dust grains $u_{i0} = u_{d0} = 0$. And, secondly we have considered the viscous coefficients for both the species. Basically, the kinematic viscosity is the origin of this type of dispersion relation and with the increase of the viscous coefficient the value of ω'' will increase with the increase of k_i . Also from figure 2 we can say that the finite temperature coefficient of ions σ plays a pivotal role in the imaginary dispersion relation with the increase of the finite temperature coefficient of ions the value of ω'' will decrease with the increase of k_i .

Now, in this section we will discuss parametric dependence of the different wave structures. Firstly, in figure 3, we discuss the variation of the shock wave for different Mach number (M) but all the other plasma quantities are constant. When the Mach number, i.e., the value of the frame velocity increases the width and the amplitude of the shock fronts increase. It is clear that the nonlinear and dissipative coefficients A and C have negative values, and the value of these decreases with the growth of the Mach number. On the other hand, the dispersive coefficient B is positive, and this coefficient B increases

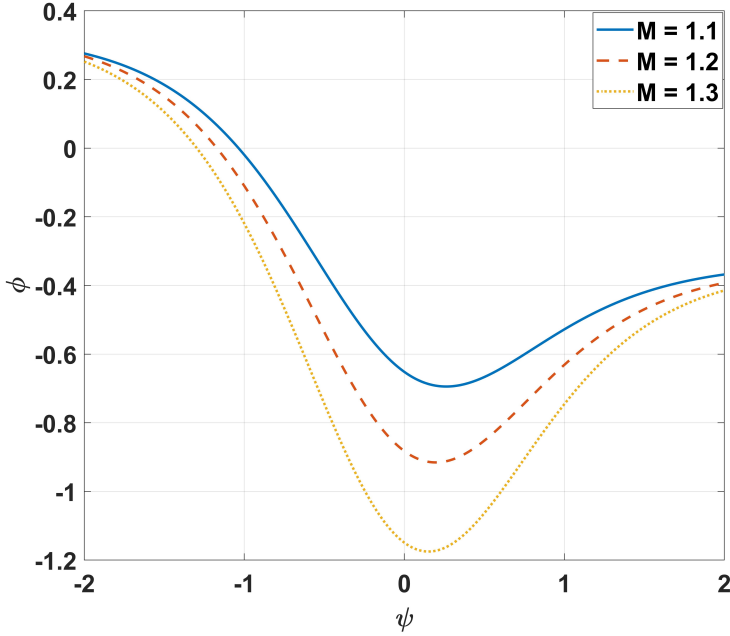


Fig. 3 Shock for different Mach numbers (M) with unperturbed ion streaming velocity(u_{i0}) = 0.3, unperturbed dust streaming velocity(u_{d0}) = 0.07, kinematic viscosity of ion (η_{i0}) = 0.09, kinematic viscosity of dust (η_{d0}) = 0.07, finite temperature coefficient (σ) = 0.65, kappa index (κ) = 5 and dust charge (q) = 1

with the increment of the Mach number. This result can also be explained physically as when the wave frame velocity is high that means the dust-ion acoustic waves propagate faster in the medium then it can have very little time to form the non-linearity but the medium also has the little time to apply the existing dissipation on it. Whereas the fastness of that same waves increases the dispersive nature of the medium. In figure 4, we discuss the variation of the shock wave for different finite temperature coefficient (σ) with all the other quantities remain constant. This is basically a degeneracy parameter and discussion of it is a little bit difficult. Here, the increase of this parameter σ the non-linearity of the shock waves decreases but the dispersive and dissipation coefficient both increases. But it is clearly seen that for lower value of the degeneracy parameter σ has very significant effect in all these three parameters but with the increase of the value of σ the dependence decreases very sharply. For an example, we can say that with the values of the other plasma parameters given in the figure 4, the change of the parameter σ from 0.55 to 0.65, the nonlinear, dispersive, and dissipation coefficients change from -6.1131 to -2.6796 , 0.0539 to 0.1504 , and -0.0721 to -0.2818 but when the parameter σ from 0.65 to 0.75 the nonlinear, dispersive, and dissipation coefficients change from -2.6796 to -2.6496 , 0.1504 to 0.1802 , and -0.2818 to -0.3464 . This happens as we consider the supersonic shock region (discussed in the discussion of figure 9) and

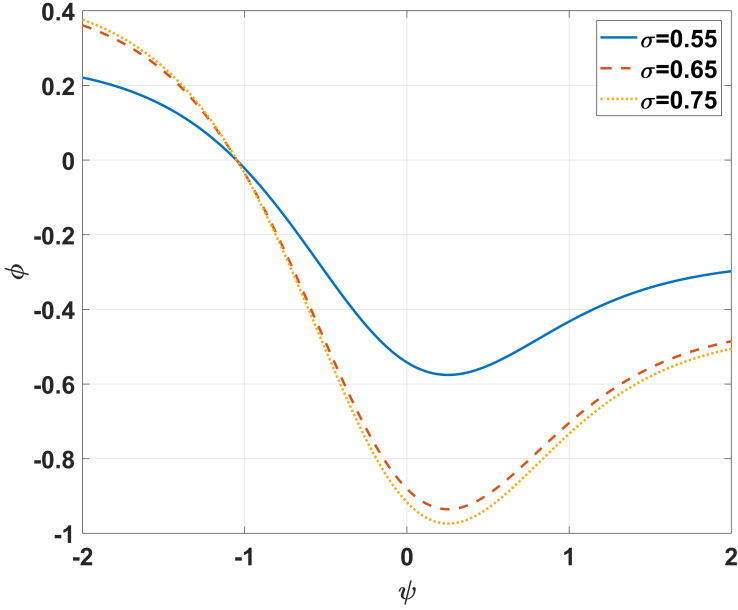


Fig. 4 Shock for different finite temperature coefficients (σ) with unperturbed ion streaming velocity(u_{i0}) = 0.3, unperturbed dust streaming velocity(u_{d0}) = 0.07, kinematic viscosity of ion (η_{i0}) = 0.09, kinematic viscosity of dust (η_{d0}) = 0.07, Mach number (M) = 1.2, kappa index (κ) = 5 and dust charge (q) = 1

the unperturbed ion velocity is higher than the unperturbed dust velocity so the effect of degeneracy parameter σ become less significant when the value of it is sufficiently higher than the critical value i.e. $\sigma_c = \frac{(M-u_{i0})^2}{3}$. Next we will discuss about the change of the shock profile for various unperturbed velocities of the charge negative dust particles and it is given in the figure 5. Dust particles are comparatively heavier than that of the ions. In this whole discussion we have considered the ion velocity more or less than ten times greater than the velocity of dust particles. As we said in the previous result that we have discussed most of the results in the supersonic region so the effect of the dust streaming velocity is very less but it is the opposite of the result that previously found for electro-static[17] or electron-acoustic [47, 48] cases. In these previous cases, when the streaming velocity of dust increases the nonlinearity decreases and dispersive effect increases significantly but in this case though the nonlinearity decreases with the increase of streaming velocity of dust particles but this change is not significant and the effect of this is contoured by decrease of the dispersive coefficient and also the increase of dissipative coefficient in formation of the shock profile. Now we will discuss about the change in the shock profile due to change in the kinematic viscosity of dust particle in figure 6. It is very clear from eq. 34 that there will be no change in A or B due to change in viscous coefficient the only changes happen in the coefficient C . The dust viscous coefficient is the main reason of the shock formation in

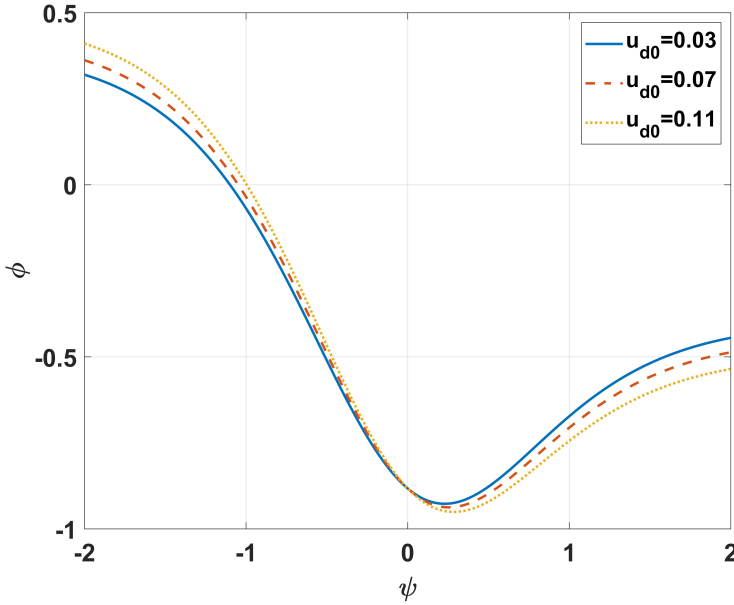


Fig. 5 Shock for different unperturbed dust streaming velocities (u_{d0}) with unperturbed ion streaming velocity (u_{i0}) = 0.3, kinematic viscosity of dust (η_{d0}) = 0.07, kinematic viscosity of ion (η_{i0}) = 0.09, finite temperature coefficient (σ) = 0.65, Mach number (M) = 1.2, kappa index (κ) = 5 and dust charge (q) = 1

a dust-ion acoustic waves because in light of physically acceptable values in supersonic wave region $\frac{\eta_{i0}(M-u_{i0})\delta}{[(M-u_{i0})^2-3\sigma]^2} < \frac{\eta_{d0}q^2}{(M-u_{d0})^3}$. In figure 7 we will see the change of shock profile due to different supra-thermal coefficient (κ). For the existence of shock or solitary profile the value of this supra-thermal coefficient κ must be greater than $\frac{3}{2}$, that is why we have taken all the values of κ greater than this value. Also, when we are taking the values of κ from 2.5–7.5, we keep in mind the Ulysses, Cluster and Helios observation for slow SW e^- [51, 52]. In this case, the dispersive and dissipative coefficient of the shock are remained constant, the only changes can happen in the nonlinear coefficient and this thing is also clear from eq. 34. It is well known that the Kappa parameter is measure of the discreteness of plasma concentration in space plasma, that is why increase of kappa parameter influences the greater shock. Two fluids can produce shock by propagating along side or colliding to each other. There are two kinds of shock that can form in case of fluids the first and mostly found in a viscous plasma is the strong shock when two fluids are propagating or colliding with each other with a velocity greater than the local acoustic waves, i.e. ($M > 1$) and the second kind of shock when two fluids collide a subsonic speed ($M < 1$) which is known as weak shock, this type of shock is very well known in case of fluids [53, 54] and for laser plasma interaction [17] but till now no report has been made in the case of dusty plasma. In figures 8, we have discussed the transition of weak to strong shock and in figure 9, we have shown

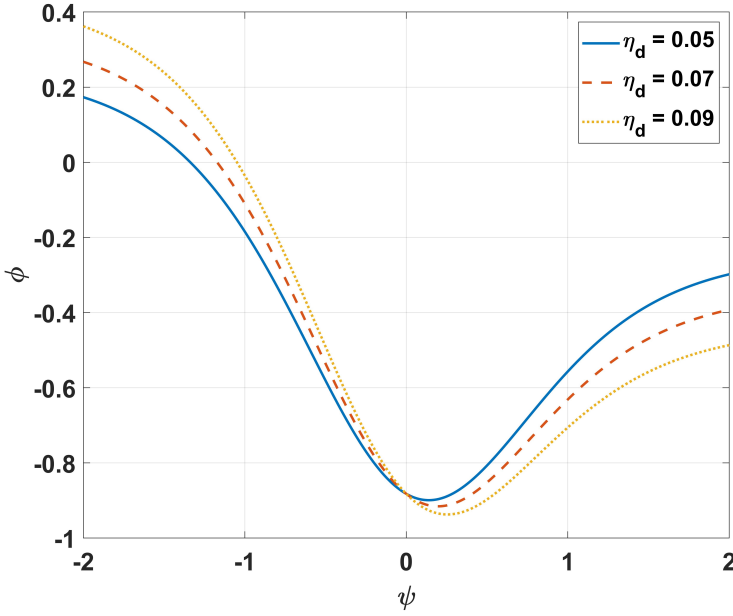


Fig. 6 Shock for different kinematic viscosity of dust (η_{d0}) with unperturbed ion streaming velocity(u_{i0}) = 0.3, unperturbed dust streaming velocity(u_{d0}) = 0.07, kinematic viscosity of ion (η_{i0}) = 0.09, finite temperature coefficient (σ) = 0.65, Mach number (M) = 1.2, kappa index (κ) = 5 and dust charge (q) = 1

two different kinds of shock for subsonic ($M = 0.7$) and supersonic ($M = 1.2$) frame velocity.

Now as we have discussed in the section 4.2 when there is no viscous term the KdVB transforms into KdV equation and here we will discuss the analytical solution of KdV equation, i.e the solitary waves. In figure 10, we can see that with an increase in the Mach Number (M), the nonlinearity and dispersive coefficient decrease and increase, respectively. This has the same effect as we have seen in case of the figure 3. In this case and also in the figure 3, the Mach number (M) also has a critical value i.e. $M_c = 1.3$. Greater than this value ($M > M_c$) the polarity of the shock waves as well as the solitary waves will change, that means all these rarefactive shock and solitary wave structures become compressive beyond this value of M . In the figure 11, we have discussed the variation of solitary profile for different finite temperature degeneracy parameters (σ). Initially, the nonlinear coefficient decreases and dispersive & dissipation coefficient increases with the increase of the finite temperature degeneracy parameter. When the degeneracy parameter σ increases greater than 0.661 the nonlinear coefficient starts to increase along with other two parameters and that is why there is a different tendency of the solitary waves and this is same for cases of the shock waves too as shown in the figure 4. Now, in the figure 12, we see that the streaming velocity of dust cannot alter the width but increases the amplitude of the solitary wave. This has happened

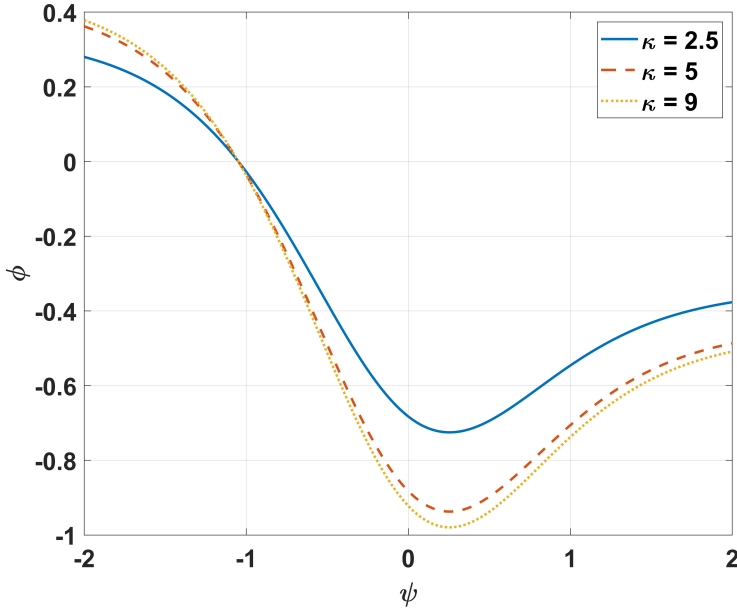


Fig. 7 Shock for different kappa indices (κ) with unperturbed ion streaming velocity(u_{i0}) = 0.3, unperturbed dust streaming velocity(u_{d0}) = 0.07, kinematic viscosity of dust (η_{d0}) = 0.07, kinematic viscosity of ion (η_{i0}) = 0.09, finite temperature coefficient (σ) = 0.65, Mach number (M) = 1.2, and dust charge (q) = 1

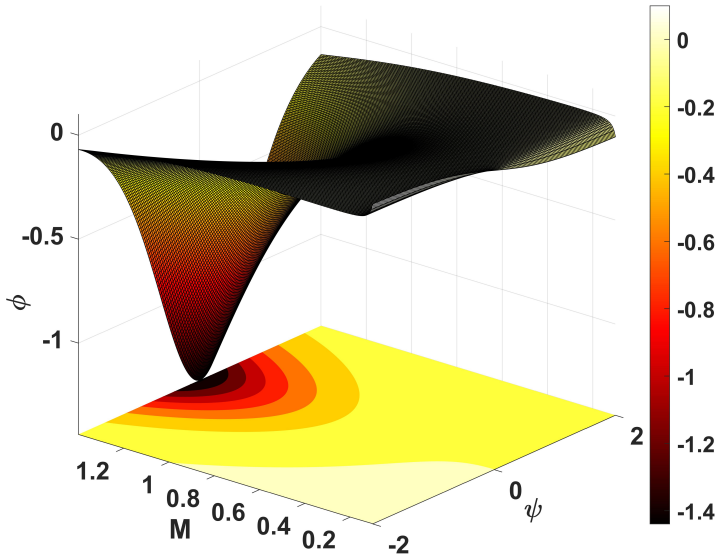


Fig. 8 Transition from Weak to Strong Shock Region

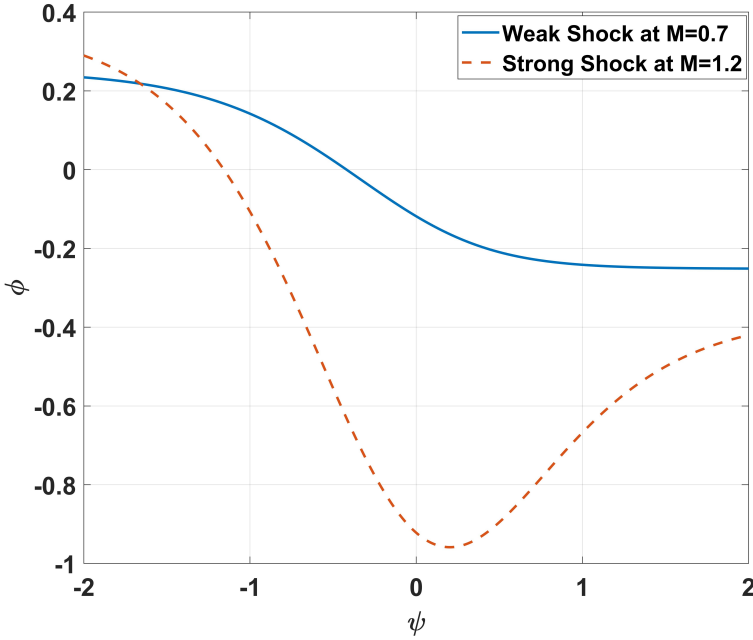


Fig. 9 Weak and Strong Shock

due to simultaneous decrease of the nonlinear and dispersive coefficient of the solitary wave with the increase of dust streaming velocity.

In figure 13, we have discussed the formation and variation of solitary profile for various supra-thermal parameters (κ). From equation 34, it is very clear that the only coefficient that is affected by supra-thermal parameter (κ) is the nonlinear coefficient A and it has a decreasing tendency with the increasing value of κ that is why the width and amplitude is increasing with the increased value of κ . Next we have shown in the figure 14 the variation of solitary profile due to different Mach numbers that is the transition of the solitary profile starting from the subsonic velocity region and ending in the supersonic velocity region for the wave. In the figure 15, we have plotted the exact solution of KdV from equation 38 and the numerical solution of the same with the help of set of equation from 39- 45. For the numerical solution, we have considered the space like steps as $\Delta\xi = 0.04$ and time like steps as $\Delta\tau = 0.05$, the maximum error in $\phi^{(1)}$ from the exact to numerical solution is 0.009152.

At last we will discuss the variation of non-linear coefficient with ion density (δ) for different supra-thermal coefficient (κ) (16) and dissipative coefficient with ion density (δ) for different viscous coefficients of dust (η_{d0}) (17). It is very much evident from equation 34 that two kinds of shock/ soliton may be possible to form. One is compressive shock/ soliton and another rarefactive shock/ soliton structures in this scenario and for that the nonlinear coefficient $A > 0$ and $A < 0$, respectively. But from figure 16, we can see the nonlinear coefficient is throughout negative that is why we are getting rarefactive shocks

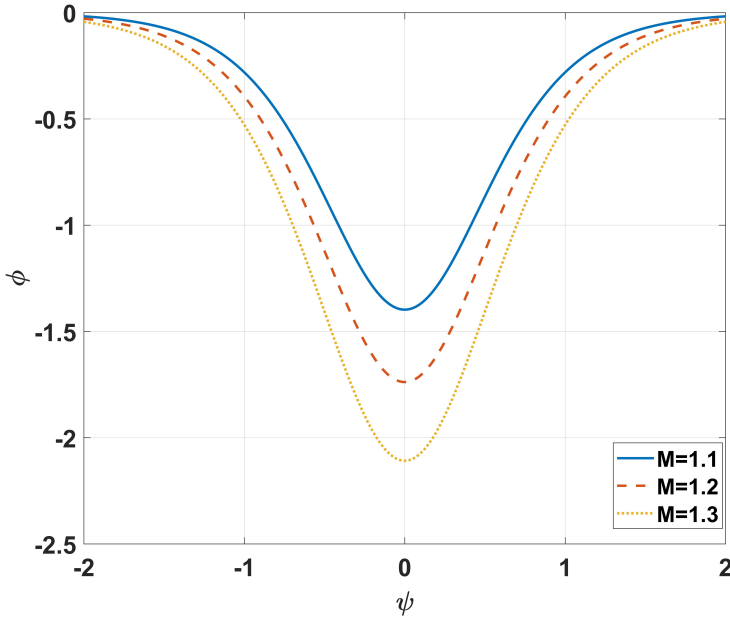


Fig. 10 Solitary for different Mach numbers (M) with unperturbed ion streaming velocity(u_{i0}) = 0.3, unperturbed dust streaming velocity(u_{i0}) = 0.07, finite temperature coefficient (σ) = 0.65, kappa index (κ) = 5 and dust charge (q) = 1

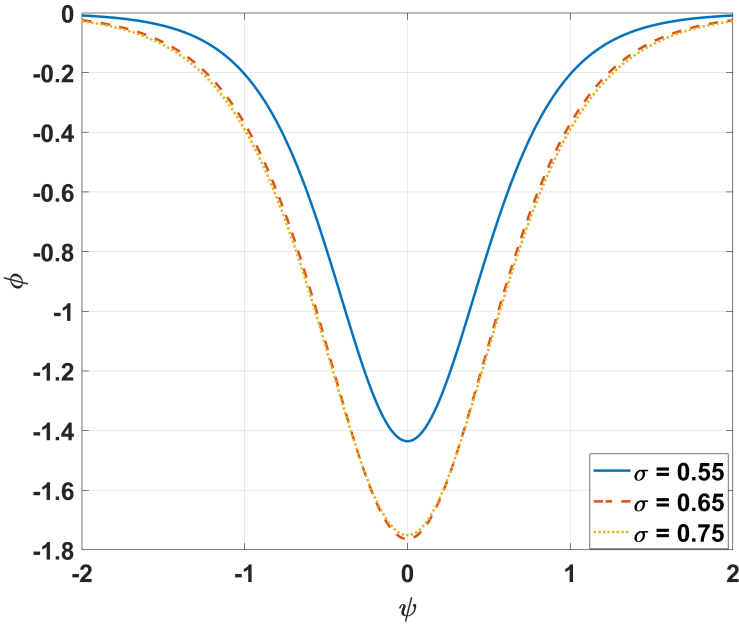


Fig. 11 Solitary for different finite temperature coefficients (σ) with unperturbed ion streaming velocity(u_{i0}) = 0.3, unperturbed dust streaming velocity(u_{i0}) = 0.07, Mach number (M) = 1.2, kappa index (κ) = 5 and dust charge (q) = 1

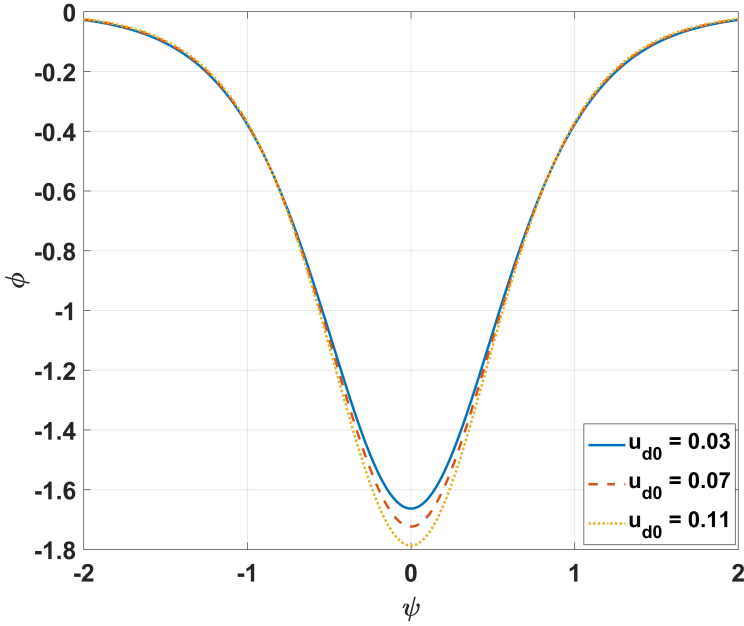


Fig. 12 Solitary for different unperturbed dust streaming velocities (u_{d0}) with unperturbed ion streaming velocity(u_{i0}) = 0.3, finite temperature coefficient (σ) = 0.65, Mach number (M) = 1.2, kappa index (κ) = 5 and dust charge (q) = 1

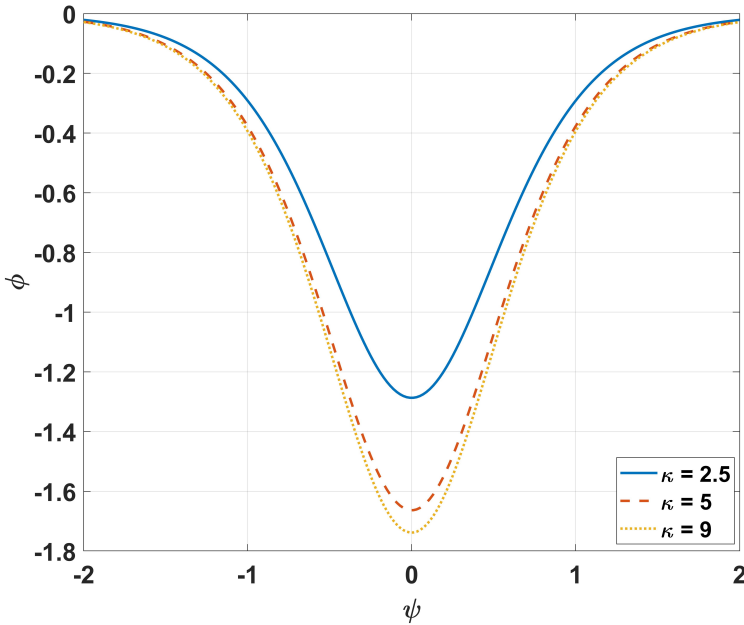


Fig. 13 Solitary for different kappa indices (κ) with unperturbed ion streaming velocity(u_{i0}) = 0.3, unperturbed dust streaming velocity(u_{d0}) = 0.07, finite temperature coefficient (σ) = 0.65, Mach number (M) = 1.2, and dust charge (q) = 1

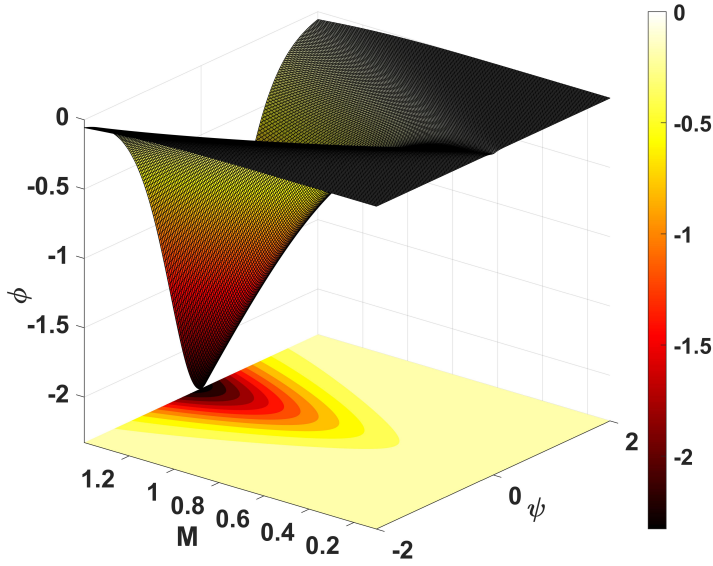


Fig. 14 Solitary 3D for different Mach Numbers (M) with unperturbed ion streaming velocity(u_{i0}) = 0.3, unperturbed dust streaming velocity(u_{d0}) = 0.07, finite temperature coefficient (σ) = 0.65, kappa index (κ) = 5 and dust charge (q) = 1

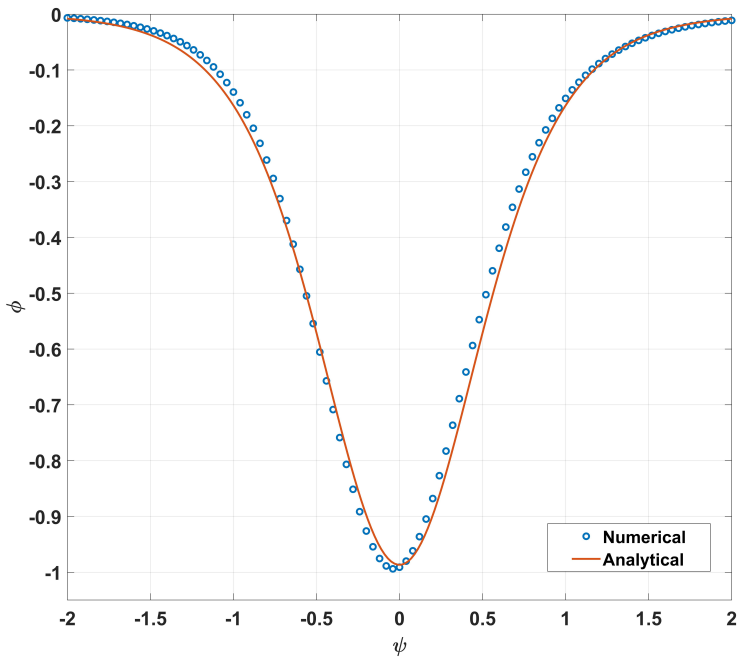


Fig. 15 Numerical and analytical KdV

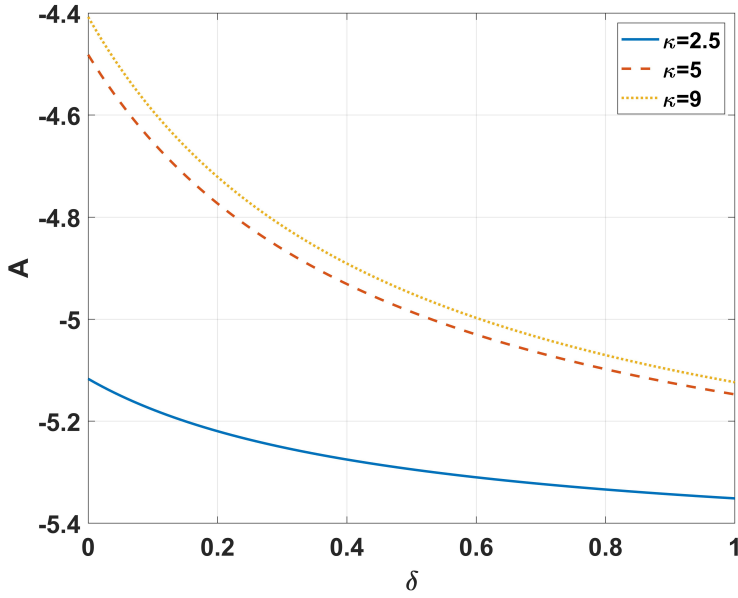


Fig. 16 Non-linear coefficient for different Kappa (κ)

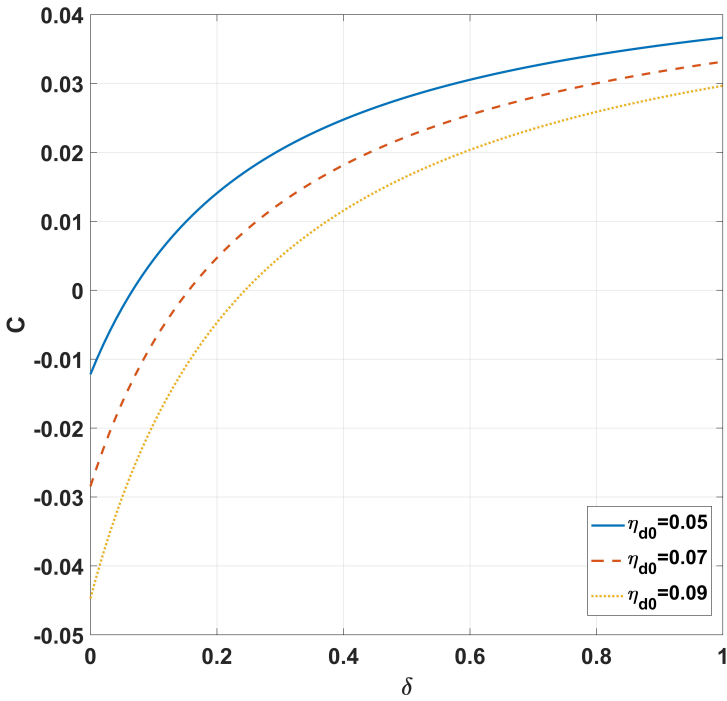


Fig. 17 Dissipative coefficient for different viscous coefficient of dust (η_{d0})

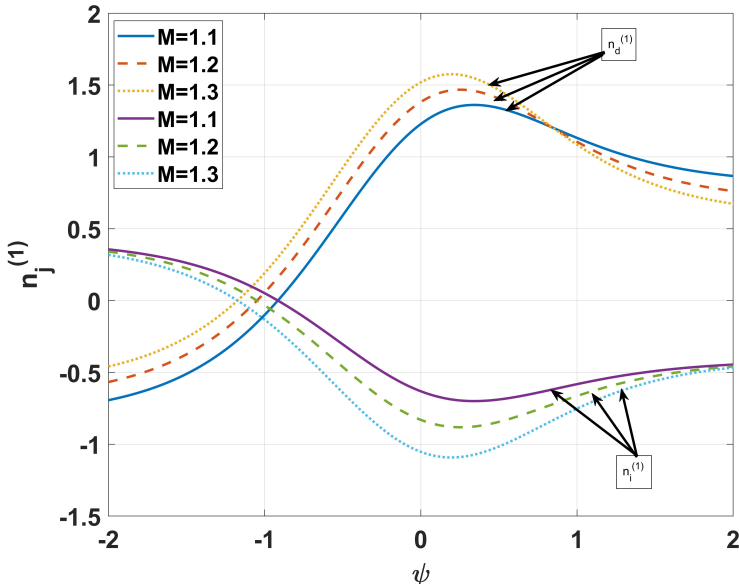


Fig. 18 First order perturbed density of dust and ion with viscosity

and solitons. Again as $\phi_0 = \frac{3M}{A}$ so due to increasing value of A will cause the decrease in the amplitude. So, this variation of A with different κ is also supported by the figures 7 and 13.

In figures 18 and 19, we have discussed the first order perturbed density change of dusts and ions in presence and absence of the viscosity with different Mach number (M). When viscous force is absent in medium (figure 19), we can see that the density of dust has a very little change with various M . This is due to heavy mass of the dust than ion, and also the density of dust and ion has different polarities. But from figure 18, we can see that the effect of viscosity has larger impact than the effect of mass as in presence of viscosity there is a sufficient amount of changes in the dust density with the change in the Mach number (M) as the viscosity considered in this paper is kinetic in nature.

The Hamiltonian $H(\phi, z)$ is given in equation 50 defines the trajectory of the phase plot is given in figure 20. In this figure 20, we can easily define two equilibrium points $E_0(0, 0)$ and $E_1(\frac{v}{A}, 0)$ of the system equation 46 as saddle point and center. The solitary wave solution 38 of equation 37 represents the homoclinic orbit of the system 46. And periodic travelling wave solution of equation 37 represents the periodic orbit of the system 46. In figure 20, the phase portrait of equation 46 is plotted. With the presence of the plasma parameters like $M = 1$, $u_{i0} = 0.3$, $u_{d0} = 0.07$, $\eta_{i0} = 0.9$, $\eta_{d0} = 0.07$, $\sigma = 0.7$ and $\kappa = 5$, we have shown the saddle point $E_0(0, 0)$ with no separatrix enclosed by the nonlinear homoclinic trajectory ($NHT_{T,0}$) which is obviously corresponds to the solitary wave solution shown in equation 37. Again around the

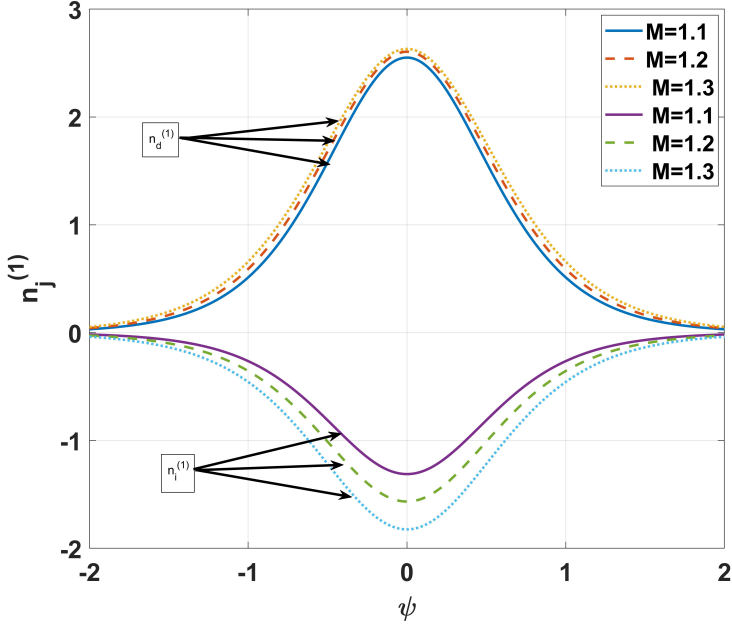


Fig. 19 First order perturbed density of dust and ion without viscosity

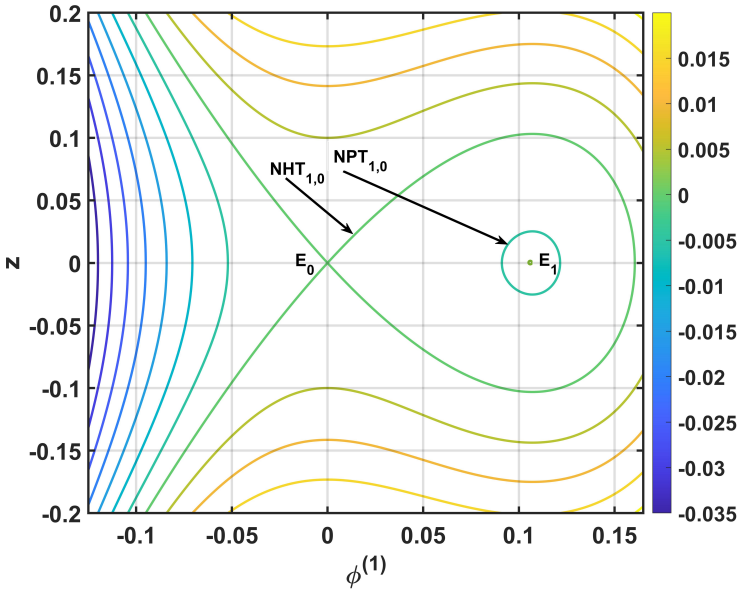


Fig. 20 Phase plot of the system (46) with unperturbed ion streaming velocity (u_{i0}) = 0.3, finite temperature coefficient (σ) = 0.65, Mach number (M) = 1.2, kappa index (κ) = 5 and dust charge (q) = 1

critical point $E_1(\frac{v}{A}, 0)$ corresponding to the periodic solution there exists the family of nonlinear periodic trajectories ($NPT_{1,0}$) [55, 56]. The corresponding analytical solution of nonlinear homoclinic trajectory ($NHT_{T,0}$) have already been shown in the figures 10-14.

7 Conclusion:

In the light of the calculation and study this paper is divided into three parts, firstly with the help of reductive perturbation technique (RPT) we analytically derived and solved the KdV-Burger and KdV equation and get the shock and solitary waves as there solution, secondly using finite difference method we have done the numerical solution of KdV and lastly with the help of total energy of the system when there is no dissipative force present in the system we have done the phase plane analysis.

In the model section we have discussed three things very broadly

(a) The presence of Fermi-Dirac statistics in case of ion distribution. Various astrophysical and laboratory plasmas are in this category if they follow the condition we have mentioned in the section 2.2. H^+ plasma is one of this kind of plasma.

(b) The detailed discussion of kinematic viscosity in both dust and ion species.

(c) The reason behind taking the dust charge as constant in DIA case has also been discussed in section 2.3.

In the production of shock waves the dust kinematic viscous coefficient (η_{d0}) is the most important parameter, so we are very careful in taking the value of this. From the work of Vorona *et al.* [57] we can have some ideas what value should be for this parameter and tried to follow this in the manuscript. For the figures 3-5, 7-9 and 18 we have taken the kinematic viscosity of dust $n_{d0} = 0.07$ and for figures 6 and 17 it is shown in the legends.

Keeping the above mentioned values of viscous coefficient and other physically admissible values for different plasma parameters for the numerical study we have found some of the important results that we have mentioned below.

(a) For the first time we have reported two types of shock that is weak and strong shock in a DIA mode.

(b) Also physically accepted values for the super sonic wave region is also discussed.

(c) The critical value of finite temperature degeneracy parameter σ_c have also been discussed and again what values would be physically acceptable for the supersonic wave region have been discussed.

(d) The critical value of the Mach number is also discussed in this result beyond which the polarity of shock and solitary waves would changes i.e. rarefactive shock/soliton transform in compressive shock/soliton.

If we want to verify in accordance with the result in laboratory environment we have made some changes, one of these changes is that we have to take Boltzmann distribution of electron and it can easily happened by taking very

large value of κ , as we know when $\kappa \rightarrow \infty$ the Kappa distribution transforms into Boltzmann distribution.

Acknowledgments. Authors would like to thank Prof. B. K. Saikia, Acting Centre Director, Centre of Plasma Physics – Institute for Plasma Research for providing facility and environment to produce this research article. One of the authors JG extend his heartfelt thanks to Gunjan Sharma, Rupali Paul and Kishor Deka for their valuable suggestions to improve the quality of the article.

References

- [1] Dragan, G.S., Kutarov, V.V.: Correlation function of the coupling parameter in dusty plasmas. AIP Conference Proceedings **1925**(1), 020027 (2018) <https://aip.scitation.org/doi/pdf/10.1063/1.5020415>. <https://doi.org/10.1063/1.5020415>
- [2] Patrice, D.T., Mohamadou, A., Kofane, T.C.: Nonlinear dust ion acoustic waves behaviors analysis in warm viscous dusty plasma with trapped ions. Physics of Plasmas **24**(12), 123706 (2017) <https://doi.org/10.1063/1.5017505>. <https://doi.org/10.1063/1.5017505>
- [3] Patrice, D.T., Mohamadou, A., Kofane, T.C.: Nonlinear dust ion acoustic waves behaviors analysis in warm viscous dusty plasma with trapped ions. Physics of Plasmas **24**(12), 123706 (2017)
- [4] Shukla, P.K., Mamun, A.: Introduction to dusty plasma physics. CRC press (2015)
- [5] Rao, N., Shukla, P., Yu, M.Y.: Dust-acoustic waves in dusty plasmas. Planetary and space science **38**(4), 543–546 (1990)
- [6] Shukla, P., Silin, V.: Dust ion-acoustic wave. Physica Scripta **45**(5), 508 (1992)
- [7] d’Angelo, N.: Ion-acoustic waves in dusty plasmas. Planetary and Space Science **42**(6), 507–511 (1994)
- [8] Bansal, S., Aggarwal, M., Gill, T.S.: Nonplanar ion acoustic waves in dusty plasma with two temperature electrons: Application to saturn’s e ring. Physics of Plasmas **27**(8), 083704 (2020)
- [9] Ma, J.-X., Yu, M.: Self-consistent theory of ion acoustic waves in a dusty plasma. Physics of Plasmas **1**(11), 3520–3522 (1994)
- [10] Vranješ, J., Pandey, B., Poedts, S.: Ion–acoustic waves in dusty plasma with charge fluctuations. Physics of Plasmas **9**(4), 1464–1467 (2002)

- [11] Mamun, A.A., Tasnim, S.: Dust-ion-acoustic shock and solitary waves in a dusty electronegative plasma. *Physics of Plasmas* **17**(7), 073704 (2010) <https://doi.org/10.1063/1.3464224>. <https://doi.org/10.1063/1.3464224>
- [12] Hassan, M., Biswas, S., Habib, K., Sultana, S.: Dust-ion-acoustic waves in a κ - nonthermal magnetized collisional dusty plasma with opposite polarity dust. *Results in Physics* **33**, 105106 (2022). <https://doi.org/10.1016/j.rinp.2021.105106>
- [13] Roy, K., Saha, T., Chatterjee, P.: Effect of ion kinematic viscosity on large amplitude dust ion acoustic solitary waves. *Astrophysics and Space Science* **349**(2), 745–751 (2014). <https://doi.org/10.1007/s10509-013-1625-9>
- [14] Adhikary, N.C.: Effect of viscosity on dust-ion acoustic shock wave in dusty plasma with negative ions. *Physics Letters A* **376**(17), 1460–1464 (2012). <https://doi.org/10.1016/j.physleta.2012.03.006>
- [15] Goswami, J., Chandra, S., Ghosh, B.: Study of small amplitude ion-acoustic solitary wave structures and amplitude modulation in e-p-i plasma with streaming ions. *Laser and Particle Beams* **36**(1), 136–143 (2018)
- [16] Devanandhan, S., Singh, S., Lakhina, G.: Electron acoustic solitary waves with kappa-distributed electrons. *Physica Scripta* **84**(2), 025507 (2011)
- [17] Goswami, J., Chandra, S., Sarkar, J., Chaudhuri, S., Ghosh, B.: Collisionless shocks and solitons in dense laser-produced fermi plasma. *Laser and Particle Beams* **38**(1), 25–38 (2020)
- [18] Ghosh, A., Goswami, J., Chandra, S., Das, C., Arya, Y., Chhibber, H.: Resonant interactions and chaotic excitation in nonlinear surface waves in dense plasma. *IEEE Transactions on Plasma Science* (2021)
- [19] Barkan, A., D’angelo, N., Merlino, R.: Experiments on ion-acoustic waves in dusty plasmas. *Planetary and Space Science* **44**(3), 239–242 (1996)
- [20] Nakamura, Y., Bailung, H., Shukla, P.: Observation of ion-acoustic shocks in a dusty plasma. *Physical review letters* **83**(8), 1602 (1999)
- [21] Paul, R., Sharma, G., Deka, K., Adhikari, S., Moulick, R., Kausik, S.S., Saikia, B.K.: Experimental study of charging of dust grains in the presence of energetic electrons. *Plasma Physics and Controlled Fusion* **64**(3), 035009 (2022). <https://doi.org/10.1088/1361-6587/ac44e5>
- [22] Nakamura, Y.: Experiments on ion-acoustic shock waves in a dusty plasma. *Physics of Plasmas* **9**(2), 440–445 (2002) <https://doi.org/10.1063/1.1431974>. <https://doi.org/10.1063/1.1431974>

- [23] Kaur, B., Saini, N.S.: Dust ion-acoustic shock waves in a multicomponent magnetorotating plasma. *Zeitschrift für Naturforschung A* **73**(3), 215–223 (2018). <https://doi.org/10.1515/zna-2017-0397>
- [24] Haider, M.M., Nahar, A.: Dust-Ion-Acoustic Solitary and Shock Structures in Multi-Ion Plasmas with Super-Thermal Electrons. *Zeitschrift Naturforschung Teil A* **72**(7), 627–635 (2017). <https://doi.org/10.1515/zna-2017-0108>
- [25] Denra, R., Paul, S., Sarkar, S., *et al.*: Study of the characteristics of dust acoustic solitary waves and dust acoustic shock waves in electron free dusty space plasma. *Journal of Modern Physics* **9**(05), 948 (2018)
- [26] Pierrard, V., Lazar, M.: Kappa distributions: Theory and applications in space plasmas. *Solar physics* **267**(1), 153–174 (2010)
- [27] Goswami, J., Sarkar, J., Chandra, S., Ghosh, B.: Amplitude-modulated electron-acoustic waves with bipolar ions and kappa-distributed positrons and warm electrons. *Pramana* **95**(2), 1–10 (2021)
- [28] Atteya, A., Sultana, S., Schlickeiser, R.: Dust-ion-acoustic solitary waves in magnetized plasmas with positive and negative ions: The role of electrons superthermality. *Chinese Journal of Physics* **56**(5), 1931–1939 (2018). <https://doi.org/10.1016/j.cjph.2018.09.002>
- [29] Baluku, T., Hellberg, M.: Dust acoustic solitons in plasmas with kappa-distributed electrons and/or ions. *Physics of Plasmas* **15**(12), 123705 (2008)
- [30] Liu, Z., Du, J.: Dust acoustic instability driven by drifting ions and electrons in the dust plasma with lorentzian kappa distribution. *Physics of Plasmas* **16**(12), 123707 (2009)
- [31] Nicolaou, G., Livadiotis, G., Owen, C.J., Verscharen, D., Wicks, R.T.: Determining the kappa distributions of space plasmas from observations in a limited energy range. *The Astrophysical Journal* **864**(1), 3 (2018). <https://doi.org/10.3847/1538-4357/aad45d>
- [32] El-Labany, S.K., Moslem, W.M., Safy, F.M.: Effects of two-temperature ions, magnetic field, and higher-order nonlinearity on the existence and stability of dust-acoustic solitary waves in saturn’s f ring. *Physics of Plasmas* **13**(8), 082903 (2006) <https://doi.org/10.1063/1.2336183>. <https://doi.org/10.1063/1.2336183>
- [33] Shan, S.A., Saleem, H., Sajid, M.: Streaming instabilities in multicomponent interstellar clouds. *Physics of Plasmas* **15**(7), 072904 (2008) <https://doi.org/10.1063/1.2936268>. <https://doi.org/10.1063/1.2936268>

- [34] Mann, I.: Interplanetary medium – a dusty plasma. *Advances in Space Research* **41**(1), 160–167 (2008). <https://doi.org/10.1016/j.asr.2007.04.066>
- [35] Schwadron, N., Gloeckler, G.: Pickup ions and cosmic rays from dust in the heliosphere. *Space science reviews* **130**(1), 283–291 (2007)
- [36] Holzer, T.E., Leer, E., Zhao, X.-P.: Viscosity in the solar wind. *Journal of Geophysical Research: Space Physics* **91**(A4), 4126–4132 (1986). <https://doi.org/10.1029/JA091iA04p04126>
- [37] Kumar Samanta, U., Saha, A., Chatterjee, P.: Bifurcations of nonlinear ion acoustic travelling waves in the frame of a zakharov-kuznetsov equation in magnetized plasma with a kappa distributed electron. *Physics of Plasmas* **20**(5), 052111 (2013) <https://doi.org/10.1063/1.4804347>
- [38] Goswami, J., Sarkar, J.: Kbm approach to electron acoustic envelope soliton in viscous astrophysical plasma. *Physica Scripta* **96**(8), 085601 (2021)
- [39] Misra, A.P., Roy Chowdhury, K., Roy Chowdhury, A.: Saddle-node bifurcation and modulational instability associated with the pulse propagation of dust ion-acoustic waves in a viscous dusty plasma: a complex nonlinear schrödinger equation. *Physics of plasmas* **14**(1), 012110 (2007)
- [40] Sen, B., Das, B., Chatterjee, P.: Effect of electron inertia on large amplitude solitary waves in presence of kinematic viscosity in dusty plasma. *The European Physical Journal D* **49**(2), 211 (2008). <https://doi.org/10.1140/epjd/e2008-00158-3>
- [41] Akbari-Moghanjoughi, M., Eliasson, B.: Hydrodynamic theory of partially degenerate electron-hole fluids in semiconductors. *Physica Scripta* **91**(10), 105601 (2016). <https://doi.org/10.1088/0031-8949/91/10/105601>
- [42] Lifshitz, E.M., Pitaevskii, L.P.: *Statistical physics: theory of the condensed state*. Elsevier (2013)
- [43] Masood, W., Mushtaq, A., Khan, R.: Linear and nonlinear dust ion acoustic waves using the two-fluid quantum hydrodynamic model. *Physics of Plasmas* **14**(12), 123702 (2007) <https://doi.org/10.1063/1.2803775>
- [44] El-Hanbaly, A., Sallah, M., El-Shewy, E., Darweesh, H.: Kinematic dust viscosity effect on linear and nonlinear dust-acoustic waves in space dusty plasmas with nonthermal ions. *Journal of Experimental and Theoretical Physics* **121**(4), 669–679 (2015)

- [45] Shahmansouri, M.: Dissipative dust acoustic solitary waves in an electron depleted dusty plasma with superthermal ions (2013)
- [46] Chaudhuri, S., Chowdhury, A.R.: On the effect of electron streaming and existence of quasi-solitary mode in a strongly coupled quantum dusty plasma—far and near critical nonlinearity. *Plasma* **4**(3), 408–425 (2021). <https://doi.org/10.3390/plasma4030030>
- [47] Goswami, J., Chandra, S., Ghosh, B.: Shock waves and the formation of solitary structures in electron acoustic wave in inner magnetosphere plasma with relativistically degenerate particles. *Astrophysics and Space Science* **364**(4), 1–7 (2019)
- [48] Goswami, J., Chandra, S., Sarkar, J., Ghosh, B.: Electron acoustic solitary structures and shocks in dense inner magnetosphere finite temperature plasma. *Radiation Effects and Defects in Solids* **175**(9-10), 961–973 (2020)
- [49] Wazwaz, A.M.: The tanh method for travelling wave solutions to the zhiber–shabat equation and other related equations. *Communications in Nonlinear Science and Numerical Simulation* **13**(3), 584–592 (2008). <https://doi.org/10.1016/j.cnsns.2006.06.014>
- [50] Soliman, A.A., Ali, A.H.A., Raslan, K.R.: Numerical solution for the kdv equation based on similarity reductions. *Applied Mathematical Modelling* **33**(2), 1107–1115 (2009). <https://doi.org/10.1016/j.apm.2008.01.004>
- [51] Livadiotis, G.: Statistical background and properties of kappa distributions in space plasmas. *J. Geophys. Res* **120**, 1607–1619 (2015)
- [52] Štverák, Š., Maksimovic, M., Trávníček, P.M., Marsch, E., Fazakerley, A.N., Scime, E.E.: Radial evolution of nonthermal electron populations in the low-latitude solar wind: Helios, Cluster, and Ulysses Observations. *Journal of Geophysical Research (Space Physics)* **114**(A5), 05104 (2009). <https://doi.org/10.1029/2008JA013883>
- [53] Zel’dovich, Y.B., Raizer, Y.P.: *Physics of Shock Waves and High-temperature Hydrodynamic Phenomena*, pp. 45–68 (1967)
- [54] Landau, L., Lifshitz, E.: *Fluid Mechanics*. [Translated to English by J. Sykes and W. Reid]. Pergamon Press, Ltd., Oxford (1959)
- [55] Dubinov, A.E., Kolotkov, D.Y.: Ion-acoustic super solitary waves in dusty multispecies plasmas. *IEEE Transactions on Plasma Science* **40**(5), 1429–1433 (2012)
- [56] Shome, A., Banerjee, G.: Bifurcation analysis of supernonlinear waves in

an electron-positron-ion-dusty plasma having nonthermal distribution of electron and positron. *Ricerche di Matematica* (2021). <https://doi.org/10.1007/s11587-021-00634-9>

- [57] Vorona, N., Gavrikov, A., Ivanov, A., Petrov, O., Fortov, V., Shakhova, I.: Viscosity of a dusty plasma liquid. *Journal of Experimental and Theoretical Physics* **105**(4), 824–830 (2007)